

# Status of the neutrino decay solution to the solar neutrino problem

*Sandhya Choubey<sup>a \*</sup>, Srubabati Goswami<sup>a †</sup>, Debasish Majumdar<sup>b ‡</sup>*

*<sup>a</sup>Saha Institute of Nuclear Physics,*

*1/AF, Bidhannagar, Calcutta 700 064, INDIA.*

*<sup>b</sup>92 Acharya Prafulla Chandra Road, Calcutta 700 009, INDIA.*

## Abstract

We re-examine the neutrino decay solution to the solar neutrino problem in the light of the SuperKamiokande (SK) data. For the decay solution the SK spectrum data by its own can provide a fit comparable to the fit obtained from the MSW solution. However when one combines the results from the total rates of the  $^{37}\text{Cl}$  and  $^{71}\text{Ga}$  experiments the fit becomes much poorer.

PACS numbers: 14.60.Pq, 26.60.+t, 96.60.Tv, 13.35.Hb

keywords: neutrino mass, solar neutrinos, decay, mixing

---

<sup>\*</sup>sandhya@tnp.saha.ernet.in

<sup>†</sup>sruba@tnp.saha.ernet.in

<sup>‡</sup>debasish@tnp.saha.ernet.in

<sup>b</sup>Present Address: Saha Institute of Nuclear Physics, Calcutta, INDIA.

In this paper we examine the status of the neutrino decay solution to the solar neutrino problem in the light of the SK data <sup>1</sup>. Neutrino decay as a solution to the solar neutrino problem has been considered earlier (pre-SK) [3, 4, 5]. However since the Ga data implies that the low energy pp neutrinos are less suppressed compared to the high energy <sup>8</sup>B suppression seen in Cl or the Kamiokande experiments, this solution was ruled out at 99% C.L. since the decay term  $\exp(-\alpha L/E)$ , (where  $\alpha = m_2/\tau_o$ ,  $m_2$  being the mass of the unstable state and  $\tau_o$  its rest frame lifetime), suppresses the low energy neutrino flux more than the high energy flux. However the SK spectrum data shows more events for the high energy bins. Though the statistics in these high energy bins need improvement, we explore the status of the neutrino decay scenario in the context of this behaviour of the SK spectrum data.

Radiative decays of neutrinos are severely constrained [6] and thus we are interested in the non-radiative decay modes. Two classes of models have been considered in the literature in this connection.

1. In [3] neutrinos are considered to be Dirac particles. They consider the decay mode  $\nu_2 \rightarrow \bar{\nu}_{1R} + \phi$ , where  $\bar{\nu}_{1R}$  is a right handed singlet and  $\phi$  is an iso-singlet scalar. Thus all the final state particles are sterile.
2. In [4] neutrinos are assumed to be Majorana particles and the decay mode is  $\nu_2 \rightarrow \bar{\nu}_1 + J$ , where  $\bar{\nu}_1$  interacts as a  $\bar{\nu}_e$  with a probability  $|U_{e1}|^2$  and J is a Majoron.

We work with just two flavors for simplicity and assume that the state  $\nu_2$  is unstable, which decays with a rest frame lifetime  $\tau_o$ . The other neutrino mass states have lifetimes much greater than the sun-earth transit time and hence can be taken as stable. In presence of decay,

$$P_{\nu_e \nu_e} = (1 - |U_{e2}|^2)^2 + |U_{e2}|^4 \exp(-4\pi L/\lambda_d) + 2|U_{e2}|^2(1 - |U_{e2}|^2) \exp(-2\pi L/\lambda_d) \cos(2\pi L/\lambda_{osc}) \quad (1)$$

$$P_{\nu_e \nu_x} = |U_{e2}|^2(1 - |U_{e2}|^2) \{1 + \exp(-4\pi L/\lambda_d) - 2 \exp(-2\pi L/\lambda_d) \cos(2\pi L/\lambda_{osc})\} \quad (2)$$

where  $x$  can be either  $\mu$  or  $\tau$  in the two flavour framework.  $\lambda_d$  is the decay length defined as,

$$\lambda_d = 2.5 \times 10^{-3} km \frac{E}{MeV} \frac{eV^2}{\alpha} \quad (3)$$

---

<sup>1</sup>The possibility of neutrino decay as a solution to the atmospheric neutrino problem has been considered recently in [1, 2]

$\lambda_{osc}$  is the oscillation wavelength defined as

$$\lambda_{osc} = 2.5 \times 10^{-3} km \frac{E}{MeV} \frac{eV^2}{\Delta m^2} \quad (4)$$

$L = R(t)(1 - r/R(t))$ ,  $r$  being the distance of the point of neutrino production from the center of the sun and  $R(t)$  is the sun-earth distance given by,

$$R(t) = R_0 \left[ 1 - \epsilon \cos(2\pi \frac{t}{T}) \right] \quad (5)$$

Here,  $R_0 = 1.49 \times 10^{13}$  cm is the mean sun-earth distance and  $\epsilon = 0.0167$  is the ellipticity of the earth's orbit,  $t$  is the time of the year and  $T$  is 1 year. The  $\Delta m^2$  dependent oscillations are important around  $10^{-10} - 10^{-11}$  eV<sup>2</sup>. We assume  $\Delta m^2$  to be much higher so that the cosine term averages out to zero. We further assume  $U_{e1} = \cos \theta$  and  $U_{e2} = \sin \theta$  so that the survival probability is

$$P_{\nu_e \nu_e} = \cos^4 \theta + \sin^4 \theta \exp(-4\pi L/\lambda_d) \quad (6)$$

In Fig. 1 we plot  $P_{\nu_e \nu_e}$  as a function of  $\alpha$  for  $\sin^2 \theta = 0.51$  for two illustrative values of  $\nu_e$  energies 7 and 13 MeV. For  $\alpha < 10^{-13} eV^2$ , the  $\exp(-4\pi L/\lambda_d) \approx 1$  signifying very little decay. Beyond  $\alpha = 10^{-10} eV^2$  the  $\exp(-4\pi L/\lambda_d) \approx 0$  which is the case where we have very fast decay. In both these regions the probabilities are energy independent. In the region where  $\alpha$  is around  $10^{-11} eV^2$  the probability does depend on the energy.

The details of the solar neutrino code employed for performing the  $\chi^2$ -analysis is described in [7, 8]. We use the BP98 solar model [9] as the reference SSM. We perform  $\chi^2$ -analyses

- using the total rates from  $^{37}Cl$ ,  $^{71}Ga$  and SK experiments. We incorporate the theory errors and their correlations.
- using the 825 day SK spectrum data [12] including the uncorrelated as well as the energy-bin correlated errors.
- of the combined rates and SK spectrum data

For the last two cases we vary  $X_B$  – the normalization of the  $^8B$  flux with respect to the SSM value as free parameter and determine its best-fit value.

From the fact that the neutrinos from SN1987A have not decayed on their way one gets a lower bound on the electron neutrino lifetime as  $\tau_0 > 5.7 \times 10^5 (m_{\nu_e}/eV)$  sec. However if one includes neutrino mixing then shorter lifetimes are allowed provided  $|U_{e2}|^2 < 0.81$  [10]. To be consistent with this, in our analysis we vary  $\sin^2 \theta$  in the range 0 to 0.8.

The data used for the total rates is presented in Table 1. Since SK has much higher statistics, we have not included the Kamiokande results. The results obtained for Model 1 are summarised in Table 2. For the Model 2  $\nu_2$  decays to  $\bar{\nu}_1$ , which interacts as  $\bar{\nu}_e$  with a probability  $U_{e1}^2$  and  $\bar{\nu}_x$  with a probability  $U_{e2}^2$ . We present in Table 3 the results for Model 2, where we have taken into account the  $\bar{\nu}_e - e$  and  $\bar{\nu}_x - e$  scattering in addition to the  $\nu_e - e$  scattering in SK, while for the radiochemical experiments there is no change. Since the  $n\bar{u}_1$  is degraded in energy [4] the effect is not significant.

Experiment	Chlorine	Gallium	Super-Kamiokande
$\frac{\text{Observed Rate}}{\text{BP98 Prediction}}$	$0.33 \pm 0.029$	$0.562 \pm 0.043$	$0.471 \pm 0.015$

Table 1: The ratio of the observed solar neutrino rates to the corresponding BP98 SSM predictions used in this analysis. The results are from refs. [11] and [12]. For Gallium, the weighted average of the SAGE and Gallex results has been used.

Parameters	Rates (d.o.f = 1)	Spectrum (d.o.f = 15)	Rates+Spectrum (d.o.f = 18)
$\alpha$ (eV <sup>2</sup> )	0	$4.22 \times 10^{-11}$	$3.29 \times 10^{-12}$
$\sin^2 \theta$	0.5	0.51	0.32
$X_B$	Fixed at SSM value	1.5	0.72
$\chi_{min}^2$	12.59	17.68	33.59
g.o.f	$3.88 \times 10^{-2}$ %	27.99%	1.41%

Table 2: The best-fit values of the parameters, the  $\chi_{min}^2$  and the goodness of fit (g.o.f) for Model 1.

Parameters	Rates (d.o.f = 1)	Spectrum (d.o.f = 15)	Rates+Spectrum (d.o.f = 18)
$\alpha$ (eV <sup>2</sup> )	0	$3.3 \times 10^{-11}$	$3.29 \times 10^{-12}$
$\sin^2 \theta$	0.5	0.53	0.32
$X_B$	Fixed at SSM value	1.5	0.71
$\chi_{min}^2$	11.98	17.62	33.12
g.o.f	$5.38 \times 10^{-2}$ %	28.32%	1.61%

Table 3: The best-fit values of the parameters, the  $\chi_{min}^2$  and the goodness of fit (g.o.f) for Model 2.

From the analysis of only rates data the best-fit comes in the region where  $\alpha = 0$ , implying that the neutrinos are stable. For the total rates, the low energy neutrino flux should be suppressed less which is in contradiction with the energy dependence of the exponential decay term. Thus the best fit comes in the region where the decay term goes to 1. Since the probability in this region is energy independent the quality of the fit is not good.

For the only spectrum analysis, the best-fit comes in the region where the  $\exp(-\alpha L/E)$  term is non-vanishing and the high energy neutrinos are suppressed less. Since high energy bins have more number of events, the fit is much better compared to the fit to the total rates and is comparable to the ones obtained for the MSW oscillation solution ( $\chi^2_{min} = 17.62$ ) [8]. The vacuum oscillation solution gives a better fit [7]. The best-fit values quoted in Table 2 are obtained with  $X_B$  constrained to be  $\leq 1.5$ . However if we remove the upper limit and allow  $X_B$  to take arbitrary values a slightly better fit is obtained for very high values of  $X_B$ :

- $\alpha = 6.53 \times 10^{-11} \text{ eV}^2$ ,  $\sin^2 \theta = 0.8$ ,  $X_B = 6.42$ ,  $\chi^2_{min} = 17.22$ ,  $g.o.f. = 30.41\%$

We note that the  $\alpha$  does not change much. But at higher  $X_B$  one needs a higher  $\theta$ . To understand these features, in fig. 2 we plot  $X_B$  vs  $\alpha$  for various fixed values of  $\sin^2 \theta$ . For getting this curve we determine the  $X_B$  that gives the minimum  $\chi^2$  at a particular  $\alpha$  and then repeat this exercise for  $\alpha$  varying in the range  $10^{-14} - 10^{-8} \text{ eV}^2$ . The minimum  $\chi^2$  obtained at each point of the parameter space of fig. 2 is within the 90% C.L. limit of the global  $\chi^2$  minimum. There are three regions

1. For very low values of  $\alpha$  (upto  $10^{-13} \text{ eV}^2$ ) the exponential term is 1 and  $P_{\nu_e \nu_e} = 1 - 0.5 \sin^2 2\theta$  which is the average oscillation probability. This can vary from 1 to 0.5 depending on  $\theta$ . However in 11 out of 18 bins of the SK spectrum data, the  $\text{rate}_{\text{obs}}/\text{SSM} < 0.5$  and this can be achieved only by keeping  $X_B < 1.0$ .
2. In the range  $10^{-13} - 10^{-10} \text{ eV}^2$  the exponential term contributes to the survival probability and it falls sharply with increasing  $\alpha$ . Therefore in this range  $X_B$  rises sharply as  $\alpha$  increases.
3. Beyond  $10^{-10} \text{ eV}^2$  the exponential term goes to zero and the probability is  $P_{\nu_e \nu_e} = \cos^4 \theta$ . In this zone one can achieve a probability  $< 0.5$  by adjusting  $\theta$  only and  $X_B$  does not play an important role. However if  $X_B$  is allowed to vary then for smaller values of  $\theta$  the  $X_B$  needed is low and vice-versa.

In fig. 3 we plot the  $\chi^2$  for the SK spectrum data, as a function of one of the parameters, keeping the other two unconstrained. In fig. 3a the solid(dashed) line

gives the variation of  $\chi^2$  with  $\alpha$  keeping  $X_B$  unconstrained (fixed at 1.0). If  $X_B$  is 1 then lower values of  $\alpha$  are not allowed as by varying  $\theta$  alone one cannot get a probability less than 0.5. If  $X_B$  is allowed to vary then low values of  $\alpha$  are also admissible. Higher values of  $\alpha$  are allowed for both the cases. The minimum of course comes in the region where  $\alpha \sim 10^{-11}$  eV<sup>2</sup> for which the high energy neutrino events are less suppressed.

Fig. 3b gives the variation of  $\chi^2$  with  $\sin^2 \theta$  keeping  $X_B$  unconstrained (solid line) and  $X_B = 1$  (dashed line). For both the curves  $\alpha$  can take any value. For  $X_B = 1$  one cannot get a good fit in the low  $\alpha$  region as discussed above and the fit goes to the high  $\alpha$  region. In this zone the probability ( $\sim \cos^4 \theta$ ) increases as we decrease  $\theta$  and this puts a lower limit on the allowed value of  $\theta$ . This can be evaded if  $X_B$  is allowed to vary, as by adjusting  $X_B$  one can get a good fit even if  $\theta$  is very low.

Fig. 3c gives the allowed range of  $X_B$  keeping the other two parameters unconstrained. From the figure we see that values of  $X_B$  below 0.4 are not allowed at 90% C.L.. As discussed,  $X_B$  plays an important role in the low and intermediate  $\alpha$  regions. In the latter zone the  $X_B$  required is high, therefore the constraints on the low values of  $X_B$  comes from the low  $\alpha$  region. In this region as we decrease  $X_B$  the number of events will decrease which can be adjusted by increasing the survival probability and the maximum value of  $P_{\nu_e \nu_e} = 1.0$  gives a lower limit on  $X_B$ . For very high values of  $X_B$  the best-fit goes in the high  $\alpha$  region where the probability is  $\sim \cos^4 \theta$ . As we increase  $X_B$  the number of events will increase which can be compensated by increasing  $\theta$ . However from SN1987A constraints  $\sin^2 \theta$  is restricted to be  $< 0.8$  and therefore beyond  $X_B = 7.2$  one does not get a good fit.

The rest frame lifetime obtained at the best-fit  $\alpha$  from the spectrum data is  $\tau_o = (m_2/\text{eV})1.54 \times 10^{-5}$  sec. This is small enough for decay to happen before neutrino decoupling in the early universe. This can increase the effective number of light neutrinos,  $N_\nu$ , from 3. However depending on the data used the upper limit on  $N_\nu$  can be 5 or 6 [13] which is consistent with the model of neutrino decay used here.

The rest frame lifetime of  $\nu_2$  is given by [1]

$$\tau_0 = \frac{16\pi}{g^2} \frac{m_2(1 + m_1/m_2)^{-2}}{\Delta m^2} \quad (7)$$

From the best-fit  $\alpha \sim 10^{-11}$  eV<sup>2</sup> and assuming  $m_2 \gg m_1$  one gets

$$g^2 \Delta m^2 \sim 16\pi 10^{-11} \quad (8)$$

If we now incorporate the bound  $g^2 < 4.5 \times 10^{-5}$  as obtained from K decay modes [14] we obtain  $\Delta m^2 > \sim 10^{-5}$  eV<sup>2</sup>, consistent with our assumption. At the best-fit

$\alpha$  the decay length for atmospheric neutrinos is  $\lambda \approx 2.5 \times 10^{11}$  km and hence they do not decay. However for  $\Delta m^2 \geq 10^{-3}$  eV<sup>2</sup> and large mixing angles there will be substantial  $\nu_e - \nu_x$  conversion in conflict with the SK atmospheric neutrino and CHOOZ data [15, 16].

In conclusion, neutrino decay solution to the solar neutrino problem is ruled out at 99.96% C.L. from the current data on total rates. For the SK spectrum data however, one can get much better fits, for  $\nu_2$  lifetimes consistent with cosmological and supernova constraints. Although the best-fit for the spectrum data comes in the region where the probability is energy dependent, if  $X_B$  is allowed to vary the  $\chi^2$  becomes flat over the entire range of parameter space. This implies that even energy independent suppression of the  $^8B$  flux is allowed. Even if  $X_B$  is fixed at 1, the decay scenario can give  $\chi^2$  comparable to the best-fit in the energy independent high  $\alpha$  regime. For the  $^8B$  flux normalisation factor a wide range  $0.4 < X_B < 7.2$  is allowed at 90% C.L. just from the SK spectral data, if neutrino decay is operative. This is much broader than the range allowed by SSM uncertainties. For the rate+spectrum analysis the decay solution is disfavoured at more than 98% C.L. even if  $X_B$  is allowed to take arbitrary values.

The authors thank A. Raychaudhuri for his involvement during the development of the solar neutrino code that has been used in this paper. They also wish to thank S. Pakvasa and K. Kar for discussions and the organisers of WHEPP-6 where this work was initiated. D.M. acknowledges financial support from the Eastern Center of Research in Astrophysics, India.

## References

- [1] V. Barger, J.G. Learned, S. Pakvasa and T.J. Weiler, Phys. Rev. Lett. **82** (1999) 2640; V. Barger *et al.* Phys. Lett. **B462** (1999) 109.
- [2] S. Choubey and S. Goswami, hep-ph/9904257 (to be published in Astroparticle Physics) and references therein.
- [3] A. Acker, S. Pakvasa and J. Pantaleone, Phys. Rev. **D 43**, (1991) R1754, **D45** (1992) R1.
- [4] A. Acker, A. Joshipura and S. Pakvasa, Phys. Lett. **B285** (1992) 371.
- [5] A. Acker and S. Pakvasa, Phys. Lett. **B320** (1994) 320.
- [6] M. Fukugita, Phys. Rev. **D36** (1987) 3817.

- [7] S. Goswami, D. Majumdar, A. Raychaudhuri, hep-ph/9909453.
- [8] S. Goswami, D. Majumdar, A. Raychaudhuri, hep-ph/0003163.
- [9] J.N. Bahcall, S. Basu, M. Pinsonneault, Phys. Lett. **B433** (1998) 1.
- [10] J. Frieman, H. Haber and K. Freese, Phys. Lett. **B200** (1988) 115.
- [11] B.T. Cleveland *et al.*, Nucl. Phys. B (Proc. Suppl.) **38** (1995) 47; W. Hampel *et al.*, (The Gallex collaboration), Phys. Lett. **B447** (1999) 127; J.N. Abdurashitov *et al.*, (The SAGE collaboration), Phys. Rev. **C60** (1999) 055801.
- [12] Y. Suzuki, Lepton-Photon '99,  
<https://www.sldnt.slac.stanford.edu/lp99/db/program.asp> .
- [13] K. Olive and D. Thomas, Astropart. Phys. **11** (1999) 403; E. Lisi, S. Sarkar and F. Villante, Phys. Rev. **D59** (1999) 123520, S. Burles, K. Nollett, J. Truran and M.S. Turner, Phys. Rev. Lett. **82** (1999) 4176.
- [14] V. Barger, W.Y. Keung and S. Pakvasa, Phys. Rev. **D25**, (1982) 907.
- [15] K. Scholberg, hep-ex/9905016.
- [16] M. Apollonio *et al.*, Phys. Lett. **B420** (1998) 397.

## Figure Captions

Fig. 1: The variation of the survival probability  $P_{\nu_e\nu_e}$  (thick lines) and the exponential decay term  $\exp(-\alpha L/E)$  (thin lines) with  $\alpha$ , for two different values of neutrino energies. The solid curves correspond to neutrino energy = 7 MeV while the dotted curves are for neutrino energy = 13 MeV. For both the cases  $\sin^2\theta$  is fixed at 0.51.

Fig. 2: The variation of  $X_B$  with  $\alpha$  for three different values of  $\sin^2\theta$  shown in the plot. Each point on these curves is obtained by keeping  $\alpha$  and  $\sin^2\theta$  fixed and determining the  $X_B$  corresponding to the minimum  $\chi^2$ .

Fig. 3: The variation of  $\chi^2$  with (a)  $\alpha$  for  $X_B$  unconstrained (solid line) and fixed at 1.0 (dashed line), while  $\sin^2\theta$  is kept unconstrained for both curves; (b)  $\sin^2\theta$  keeping both  $\alpha$  and  $X_B$  unconstrained for the solid curve and with  $\alpha$  unconstrained and  $X_B$  fixed at 1.0 for the dashed curve; (c)  $X_B$  keeping both  $\alpha$  and  $\sin^2\theta$  unconstrained. The dotted line shows the 90% C.L. limit for 3 parameters ( $\chi^2 = \chi^2_{min} + 6.25$ ) and the dash-dotted line gives the corresponding limit for 2 parameters ( $\chi^2 = \chi^2_{min} + 4.61$ ).

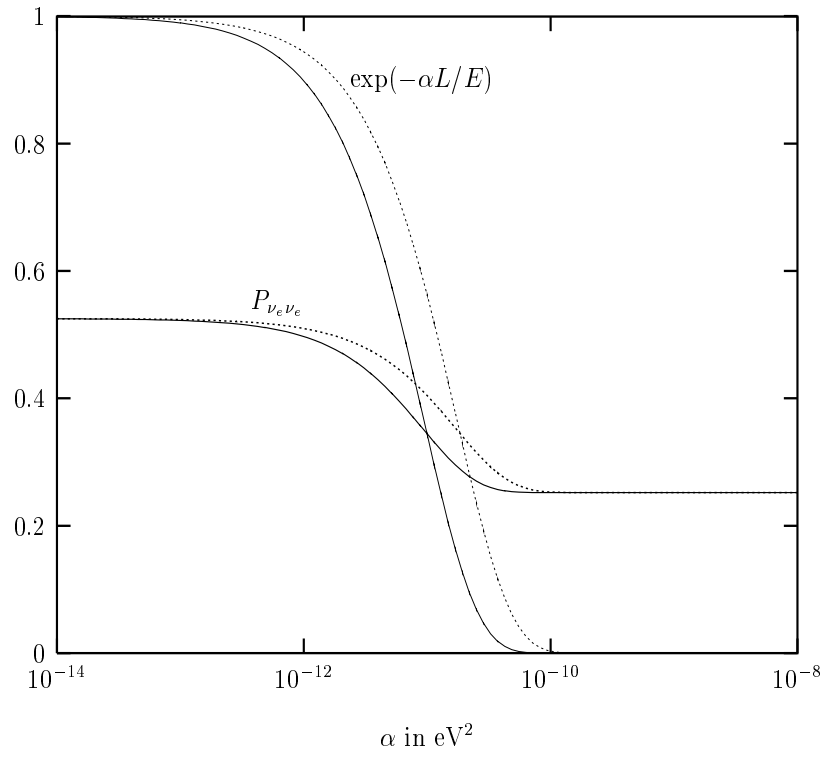


Fig. 1

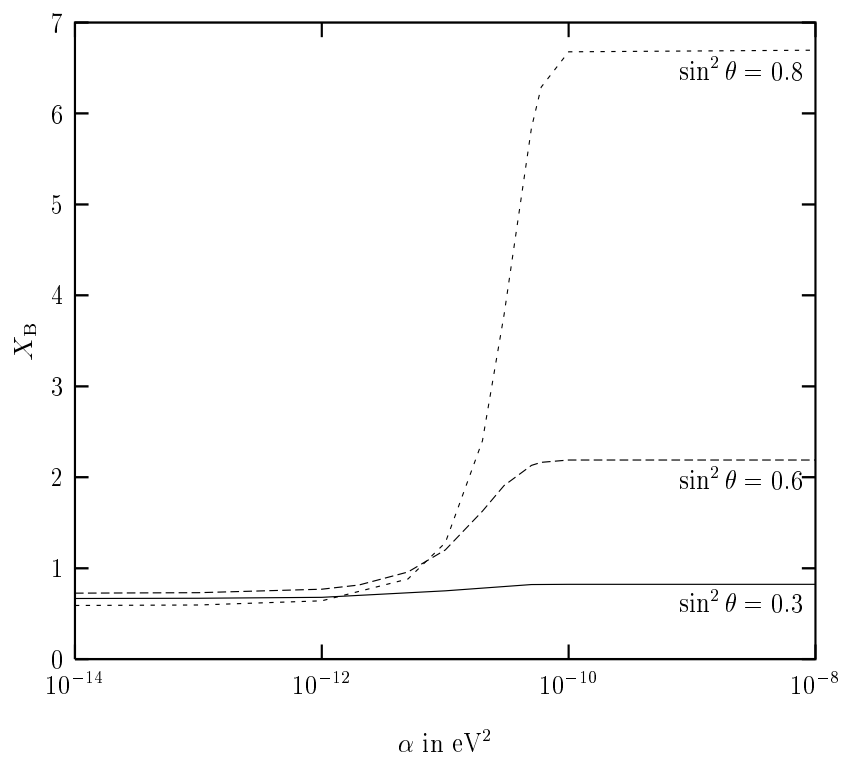


Fig. 2

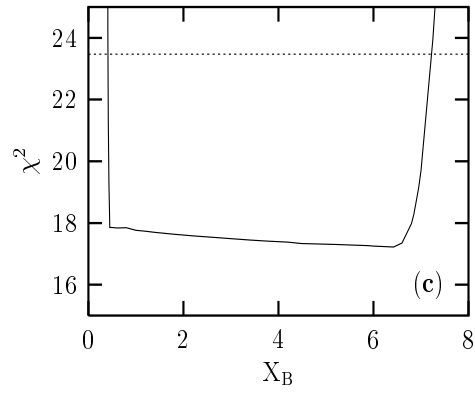
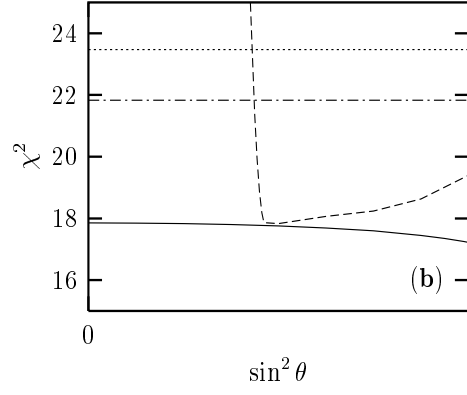
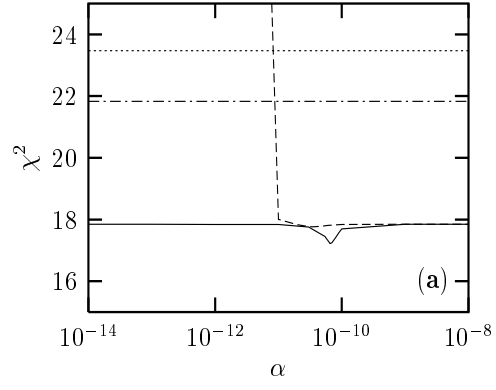


Fig. 3